



Optimization of iron-ZIF-8 catalysts for degradation of tartrazine in water by Fenton-like reaction

Ouissal Assila^a, Natália Vilaça^{a,b}, Ana R. Bertão^{a,b,c,d}, António M. Fonseca^{a,e}, Pier Parpot^{a,e}, Olívia S.G. P. Soares^{f,g}, Manuel F.R. Pereira^{f,g}, Fátima Baltazar^{c,d}, Manuel Bañobre-López^b, Isabel C. Neves^{a,e,*}

^a CQUM, Centre of Chemistry, Chemistry Department, University of Minho, Campus de Gualtar, 4710-057, Braga, Portugal

^b INL – Advanced (magnetic) Theranostic Nanostructures Lab, Nanomedicine Group, International Iberian Nanotechnology Laboratory, Av. Mestre José Veiga, 4715-330, Braga, Portugal

^c Life and Health Sciences Research Institute (ICVS), School of Medicine, University of Minho, Campus Gualtar, 4710-057, Braga, Portugal

^d ICVS/3B's – PT Government Associate Laboratory, Braga/Guimarães, Portugal

^e CEB – Centre of Biological Engineering, University of Minho, Campus de Gualtar, 4710-057, Braga, Portugal

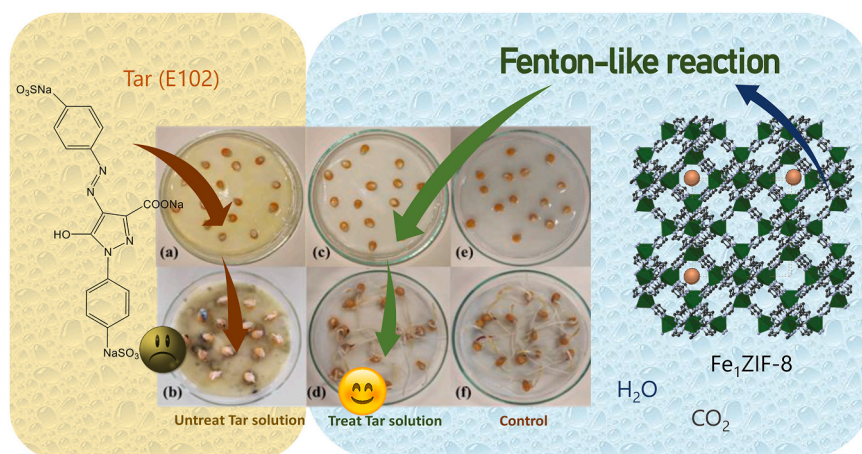
^f LSRE-LCM – Laboratory of Separation and Reaction Engineering – Laboratory of Catalysis and Materials, Faculty of Engineering, University of Porto, Portugal

^g ALiCE – Associate Laboratory in Chemical Engineering, Faculty of Engineering, University of Porto, Portugal

HIGHLIGHTS

- Synthesis of heterogeneous iron ZIF-8 catalysts.
- Fenton-like oxidation of Tartrazine with FeZIF-8 catalysts.
- Box-Behnken design: 2 g/L of Fe₁ZIF-8, T = 40 °C, t = 4h and [H₂O₂] = 12 mM.
- Higher conversion and mineralization.
- Phytotoxicity tests by germination of kernels show the success of degradation.

GRAPHICAL ABSTRACT



ARTICLE INFO

Handling Editor: Sergi Garcia-Segura

Keywords:

FeZIF-8 nanoparticles
Pollutant effluents

ABSTRACT

Optimization of iron zeolitic imidazole framework-8 (FeZIF-8) nanoparticles, as heterogeneous catalysts, were synthesized and evaluated by the Fenton-like reaction for to degrade tartrazine (Tar) in aqueous environment. To achieve this, ZIF-8 nanoparticles were modified with different iron species (Fe²⁺ or Fe₃O₄), and subsequently assessed through the Fenton-like oxidation. The effect of different parameters such as the concentration of hydrogen peroxide, the mass of catalyst and the contact time of reaction on the degradation of Tar by Fenton-like

* Corresponding author. CQUM, Centre of Chemistry, Chemistry Department, University of Minho, Campus de Gualtar, 4710-057, Braga, Portugal.

E-mail address: ineves@quimica.uminho.pt (I.C. Neves).

<https://doi.org/10.1016/j.chemosphere.2023.139634>

Received 5 June 2023; Received in revised form 21 July 2023; Accepted 22 July 2023

Available online 27 July 2023

0045-6535/© 2023 The Authors. Published by Elsevier Ltd. This is an open access article under the CC BY license (<http://creativecommons.org/licenses/by/4.0/>).

Fenton-like reaction
Mineralization
Germination rate

oxidation was studied by using the Box-Behnken design (BBD). The BBD model indicated that the optimum catalytic conditions for Fenton-like reaction with an initial pollutant concentration of 30 ppm at pH 3.0 were $T = 40\text{ }^{\circ}\text{C}$ and 12 mM of H_2O_2 , 2 g/L of catalyst and 4 h of reaction. The maximum Tar conversion value achieved with the best catalyst, $\text{Fe}_1\text{ZIF-8}$, was 66.5% with high mineralization (in terms of decrease of total organic carbon – TOC), 44.2%. To assess phytotoxicity, the germination success of corn kernels was used as an indicator in the laboratory. The results show that the catalytic oxidation by Fenton-like reaction using heterogeneous iron ZIF-8 catalysts is a viable alternative for treating contaminated effluents with organic pollutants and highlighted the importance of the validation of the optimized experimental conditions by mathematical models.

1. Introduction

Zeolitic imidazolate frameworks (ZIF), an emerging subclass of MOFs (metal organic frameworks), are porous materials similar to those of zeolites frameworks that are built by tetrahedral Si or Al and the bridging O is replaced by transition metals (such as Zn^{2+} or Co^{2+}) and are linked through N atoms in ditopic imidazolate anions, known as imidazolate linkers (Lee et al., 2015; Pan et al., 2011). Similar to zeolites, these materials can accommodate other metal species by ion exchange and present different topologies. In the ZIFs, ZIF-8 is the most widely used material in different applications (Bergaoui et al., 2021; Gao et al., 2019; Lee et al., 2015; Zhou et al., 2013). ZIF-8 ($\text{Zn}(\text{MeIM})_2$, $\text{MeIM} = 2\text{-methylimidazolate}$) present a framework comprised of 1.16 nm cages connected through six-membered windows with 0.34 nm in size, with higher thermal and chemical stability in aqueous solutions (Lee et al., 2015).

These structures are used for preparing stable heterogeneous catalysts due to their abundant functionalities, unimodal micropores, rapid electron transfer ability, and exceptional chemical and thermal stabilities to degrade organic pollutants (Ai et al., (2019); Hu et al., (2018); Liu et al., (2021); Sun et al., (2023)]. In the work of Hu et al., (2018), the catalyst ZIF-8/ Zn-Al layered double oxides was synthesized, and used for adsorption and photocatalytic degradation of methylene blue with higher performance. The degradation of bisphenol A was enhanced by the laccase encapsulation immobilized in mesoporous ZIF-8 (Ai et al., 2019). In addition, the Prussian blue analogues (PBA) were immobilized in ZIF-8 and used as heterogeneous catalyst for the degradation of Rhodamine B and the degradation efficiency of PBA-ZIF-8 was higher than that of PBA and ZIF-8 (Sun et al., 2023). In photocatalysis, the review of Liu et al. (2021) presents the successful utilization of different ZIF frameworks for visible-light-induced photocatalytic hydrogen evolution and pollutants treatment.

Recently, these materials have been used as heterogeneous catalysts for the Fenton reaction, since the ligand 2-methylimidazolate has abundant π -electron delocalization (Wang et al., 2020; Zhang et al., 2021). After the introduction of iron, ZIF-8 can provide electrons to the former substance acting as an electron donor, promoting the decomposition of hydrogen peroxide (H_2O_2) into more radical hydroxyls (OH^{\bullet}) for enhanced pollutant degradation (Wang et al., 2020). The work of Wang et al. (2020) reported that the heterogeneous catalyst ZIF-8/ MnFe_2O_4 is active in photo-Fenton degradation of tetracycline with an efficiency of 40% compared to the pristine MnFe_2O_4 . The work of Zhang et al. (2021) studied the degradation of sulfadiazine via hydrogen peroxide activation in the presence of a magnetic core-shell $\text{Fe}_3\text{O}_4@ \text{CuS}$ in ZIF-8 structure and showed that the catalysts are very active.

In this work, we report the degradation of tartrazine (Tar), a food-colouring compound known as E102, currently used in detergents due to its yellow colour by Fenton-like reaction using the heterogeneous catalysts based on ZIF-8. Tar is an azo dye compound cheaper than beta-carotene and used as an alternative to achieve similar colour, in medicinal products such as capsule shells, syrups and cosmetics (Alcantara-Cobos et al., 2020; Ouassif et al., 2020). Due to the presence of $-\text{SO}_3\text{Na}$ groups, the molecule is soluble in water and is found in several industrial effluents as a contaminant (Arabzadeh et al., 2014). For that,

four samples with iron species were prepared using ZIF-8 nanoparticles as support, two with different amounts of iron (Fe^{2+}) and two others with Fe_3O_4 species. After the selection of the best catalyst, a Box-Behnken Design (BBD) model combined with a response surface methodology (RSM) analysis was adopted in this work to determine the influence of operating conditions in the Fenton-like reaction by the evaluation of the correlation of the concentration of hydrogen peroxide, the mass of catalyst and the contact time of reaction. The choice of the BBD model is due to the capacity to create experiments economically feasible and beneficial for the optimization of different organic matter treatment processes (Assila et al., 2023). In addition, the stability of the best catalyst, the quantification of hydrogen peroxide during the reaction, the identification of the intermediate products that remain in the treated effluent and their toxicity by germination rate of grains of corn kernels were also studied.

2. Experimental section

2.1. Materials and reagents

All the reagents used for the synthesis of the several ZIF-8 nanoparticles were reagent grade and were provided by Merck. The other compounds: Sigma Aldrich provided tartrazine (Tar, $\text{C}_{16}\text{H}_9\text{N}_4\text{Na}_3\text{O}_9\text{S}_2 \geq 90\%$), sodium bisulfite (Na_2SO_3), hydrochloric acid (HCl, $\geq 99.5\%$), sodium hydroxide (NaOH, $\geq 99.0\%$) and absolute ethanol ($\text{C}_2\text{H}_5\text{OH}$, $\geq 99.7\%$). Hydrogen peroxide (H_2O_2 , 30 wt%), phosphoric acid (H_3PO_4 , analytical reagent, $\geq 85\%$), potassium titanium (IV) oxalate ($\text{K}_2\text{TiO}(\text{C}_2\text{O}_4)_2 \cdot 2\text{H}_2\text{O}$) and oxalic acid ($\text{C}_2\text{H}_2\text{O}_4$, $\geq 99.5\%$) from Merck were used as received. Deionized water was produced with an ultrapure water system (Milli-Q, EQ 7000).

2.2. Synthesis of the heterogeneous ZIF-8 catalysts and characterization

Several ZIF-8 samples were prepared in order to obtain the heterogeneous catalysts for use in the degradation of tartrazine by the Fenton-like reaction. Therefore, four samples with different iron amounts were prepared and compared to the pristine ZIF-8 nanoparticles.

Synthesis of pristine ZIF-8 nanoparticles: The synthesis of pristine ZIF-8 was performed based on a previously described procedure, with some modifications (Lee et al., 2015; Pan et al., 2011). Briefly, 1.17 g of zinc nitrate hexahydrate ($(\text{Zn}(\text{NO}_3)_2 \cdot 6\text{H}_2\text{O})$) was dissolved in 8 mL of ultrapure water and mixed for 10 min with 22.7 g of 2-methylimidazole ($\text{C}_4\text{H}_6\text{N}_2$) was dissolved in 80 mL of ultrapure water and zinc nitrate solution was added to this solution and left to be stirred for 20 min at 500 rpm. Then, the mixture was subjected to hydrothermal treatment at $120\text{ }^{\circ}\text{C}$ for 18 h. Afterwards, the solution was centrifuged at 8000 rpm for 30 min to recover the product. The product was washed 4 times with water/methanol. A small part of the product was re-dispersed in water and another part of the product was dried at $65\text{ }^{\circ}\text{C}$ overnight in a drying oven.

Synthesis of $\text{Fe}_1\text{ZIF-8}$ (80 Zn:20 Fe) nanoparticles: To perform this synthesis, two different solutions were prepared. Solution A, 2.347 g of zinc nitrate hexahydrate ($(\text{Zn}(\text{NO}_3)_2 \cdot 6\text{H}_2\text{O})$) and 0.586 g of iron (II) chloride tetrahydrate ($\text{FeCl}_2 \cdot 4\text{H}_2\text{O}$) were dissolved in 8 mL of ultrapure water and solution B, 6.486 g of 2-methylimidazole was dissolved in 80

mL of water and stirred until complete dissolution. Solution A was added to solution B and stirred for 30 min. The final solution was centrifuged at 8000 rpm for 15 min to recover the solid sample and the sample was washed 5 times with water, and dried under vacuum.

Synthesis of Fe₂ZIF-8 (50 Zn:50 Fe) nanoparticles: A solution of 1.465 g of zinc nitrate hexahydrate and 1.465 g of iron (II) chloride tetrahydrate in 8 mL of ultrapure water was prepared. This solution was mixed with 6.486 g of 2-methylimidazole dissolved in 80 mL of water and stirred for 30 min. The solid sample was recovered by centrifugation at 8000 rpm, for 15 min and washed 5 times with water, and dried under vacuum.

Synthesis of Fe₃O₄-ZIF-8 nanoparticles: 22.7 g of 2-methylimidazole was dissolved in 80 mL of ultrapure water and stirred until complete dissolution. This solution was then mixed with a solution of 1.17 g of zinc nitrate hexahydrate in 8 mL of ultrapure water and stirred for 10 min. Then, 4 mL of Fe₃O₄ nanoparticles were added to the solution and stirred for 3 h at 50 °C. The solution was centrifuged for 15 min at 8000 rpm and the solid sample was washed 5 times with ethanol, and dried under vacuum.

Synthesis of PAA-Fe₃O₄-ZIF-8 nanoparticles: For these nanoparticles, two steps were carried out. First, the synthesis of PAA-Fe₃O₄, polyacrylic acid (PAA)-grafted to Fe₃O₄ nanoparticles - A solution of 0.53 g of FeCl₂·4H₂O and 1.26 g FeCl₃·6H₂O in 5 mL of ultrapure was prepared. 0.67 g of PAA was dissolved in 2 mL of H₂O and the ferrous solution was mixed with PAA solution. Under agitation, NH₄OH was added to the mixture and a black precipitate was immediately formed. Then, the mixture was subjected to hydrothermal treatment at 150 °C, for 24 h. The solution was cooled to room temperature (RT) and nanoparticles were separated by centrifugation, rinsed with ultrapure water and acetone 5 times, and finally dispersed in ultrapure water. (ii) Synthesis of PAA-Fe₃O₄-ZIF-8 nanoparticles - A solution of 5.665 g of 2-methylimidazole in 22.9 mL of ultrapure water was prepared and stirred. Then, 2.5 mL of a solution of PAA-Fe₃O₄ was added and placed in an ultrasonic bath for 20 min plus 15 min at 400 rpm. A solution of 0.417 g of zinc nitrate hexahydrate was prepared, loaded in a syringe, and added drop by drop to the above solution over 11 min to produce the nanoparticles. The sample of the reaction was separated by centrifugation, washed 5 times with ultrapure water, and dried under vacuum.

Morphological characterization of the synthesized nanoparticles was obtained by transmission electron microscopy (TEM) measurements by means of JEOL 2100 microscope worked at 200 kV. Powder XRD patterns were acquired with a PANalytical X'Pert PRO diffractometer with Ni filtered Cu K α radiation and a PIXcel 3D detector, set at an accelerating voltage of 45 kV, and a tube current of 40 mA at RT. PANalytical High Score software was used to analyze the data.

The stability and reusability of the catalyst were characterized using energy-dispersive X-ray spectroscopy (EDX) coupled at a scanning electron microscope (SEM/EDX, FORMAT JEOL/EO). In order to avoid surface charging, samples were coated with gold in vacuum prior to analysis, by using a Fisons Instruments SC502 sputter coater.

Fourier Transform Infrared, FTIR, spectroscopy measurements of the samples were carried out using a PerkinElmer Spectrum Two spectrometer, equipped with an ATR accessory. A diamond prism was used as the waveguide. All spectra were recorded with a resolution of 4 cm⁻¹ in the wavelength region 4000-400 cm⁻¹ by averaging 16 scans and the analyses were carried out at RT.

2.3. Fenton-like reaction and experimental design

Temperature and pH used in the Fenton-like reaction for the degradation of Tar (40 °C and 3.0, respectively) were fixed at the best values found in a preliminary study in a semi-batch reactor and atmospheric pressure under stirring according to the conditions described (Assila et al., 2023). The catalysts were pre-treated at 100 °C for 2 h in an oven before the catalytic tests, in order to remove the physical water adsorbed on the surface of the nanoparticles. Previously, a screening assay was

carried out with all prepared heterogeneous ZIF-8 catalysts using the adapted catalytic conditions described in (Santos et al., 2021): 20 mg_{catalyst}/25 mL_{Tar} (30 ppm), 0.5 mL of H₂O₂ at 12 mM of concentration, T = 40 °C, pH = 3 under stirring at 300 rpm, during 4 h. The catalyst selected in this screening was used as one of the fixed parameter for the Box-Behnken Design (BBD) model.

So, the semi-batch reactor was fed with 250 mL of a Tar solution (30 ppm), at pH = 3 using 5 mL of H₂O₂, 40 °C of temperature with a specific mass of the catalyst, concentration of hydrogen peroxide and contact time under stirring at 300 rpm (Table S1). Periodically, samples of the treated effluent were withdrawn from the reactor and an excess of NaHSO₃ was added to the samples, to instantaneously consumes the remaining H₂O₂ and stop the reaction (Rodrigues et al., 2021). After centrifugation of the samples, the solution was analysed to quantify the Tar degradation by UV-vis. Catalytic tests were performed in duplicate, and the maximum deviation observed in the degradation of Tar was 2%. At the end of the reaction, the final solution after centrifugation was used to measure the concentration of Tar, total organic carbon (TOC), hydrogen peroxide and iron eventually leached out from the catalyst.

The stability of the catalyst in Tar degradation was studied using the optimum experimental catalytic conditions as described above. Four cycles were performed, after each cycle the catalyst was filtered-off, washed with ethanol, and dried in an oven at 70 °C overnight before being reused. FTIR and EDX analyses were used to verify the stability of the ZIF-8 structure and the leaching of metals after the cycle reactions.

Box-Behnken Design (BBD) model was applied to optimize the concentration of hydrogen peroxide, the mass of catalyst and the contact time of reaction, as well as to evaluate the correlation among these three variables. Thus, for BBD, it was necessary to do fifteen experiments, in which the three variables were codified in three levels, varying within the following ranges: concentration of hydrogen peroxide (X₁: 12–90 mM), mass of catalyst (X₂: 20–50 mg) and contact time of reaction (X₃: 2–6 h). The catalyst selected was Fe₁ZIF-8 after the screening tests in tartrazine (Tar) degradation by the Fenton-like reaction. So, these three variables were used to determine the model coefficient in quadratic terms (Table S1). The predicted response, Y_m, represents the variables of Tar (Y₁), equation (1):

$$Y = \beta_0 + \sum_{i=1}^k \beta_i X_i + \sum_{i=1}^{k-1} \sum_{j=2}^k \beta_{ij} X_i X_j + \sum_{i=1}^k \beta_{ii} X_i^2 + \varepsilon \quad (\text{Eq. 1})$$

where, β_0 is the intercept coefficient; β_i , β_{ii} and β_{ij} (i = 1, 2, 3; j = 1, 2, 3) are the linear, squared, and interaction coefficients, respectively. X_i and X_j are the coded independent variables and ε is the random error (Assila et al., 2023). Table S2 provides the matrix for a predictable number of experimental runs to obtain responses in terms of Tar conversion, with the number of the optimized factors k equal to three variables and C₀ is the central value, equation (2) (Assila et al., 2023).

$$N = 2 \times k \times (k - 1) + C_0 \quad (\text{Eq. 2})$$

Statistical validation was obtained using the ANOVA test at 95% confidence level.

2.4. Analytical methods

The concentration of tartrazine during the reaction was measured by UV-vis spectroscopy at $\lambda_{\text{max}} = 427$ nm, the characteristic wavelength of Tar, using a UV-vis Spectrophotometer UV-2501PC from Shimadzu. The values of the Tar concentration were obtained by the interpolation of the absorbance values at different times of reaction in the calibration curve. As well as, the concentration of hydrogen peroxide at the end of the reaction was measured by the colorimetric method, due to the formation of a yellow-orange complex formed from the reaction between H₂O₂ and potassium titanium oxalate (0.02 M), in an acid medium (pH = 1.0) and was measured by absorbance at 400 nm (Sellers, 1980).

The total organic carbon (TOC) was determined using the NPOC

method, with Shimadzu's Total Organic Carbon Analyzer TOC-L, coupled with the ASI-L autosampler of the same brand.

The toxicity of the Tar solution after the Fenton-like reaction was evaluated by germination rate of grains of corn kernels with an adapted procedure (Sancey et al., 2011). In three Petri dishes, 15 grains of corn were placed on a filter paper disc and 5 mL of each water solution was added every day at room temperature: (i) Tar solution untreated, (ii) Tar solution treated and (iii) distilled water was a witness test for irrigation during 6 days. Petri dishes were recorded and seeds were germinated in a growth chamber under controlled conditions. The number of germinated seeds was counted daily to calculate the germination rate through the ratio of the number of germinated seeds to the number of seeds sown, expressed in percentage.

Fenton-like products from Tar degradation were identified using a HPLC-MS system (Thermo LxQ) with a C-18 (150 × 4.6 mm) column and the small molecules were identified by HPLC analysis using the same equipment described before.

3. Results and discussion

Several ZIF-8 nanoparticles were synthesized and modified with iron species to obtain stable heterogeneous catalysts for the Fenton reaction. For that, the pristine ZIF-8 nanoparticles were modified with different species of iron and the resulting nanoparticles were characterized by FTIR, TEM, XRD and analyses.

Fig. S1 shows the Fourier-transform infrared (FTIR) spectra of the different synthesized heterogeneous ZIF-8 nanoparticles and Table 1 presents the results obtained with TEM and XRD analyses.

In the IR spectrum of pristine ZIF-8, the characteristic bands attributed to the stretching vibration of the imidazole rings can be found at 600 cm^{-1} to 1500 cm^{-1} . The bands located at 1418 cm^{-1} , 1142 cm^{-1} , and 991 cm^{-1} were assigned to the stretching vibration of the C–N bond and the band at 1580 cm^{-1} corresponded to the C=N stretching vibration of the imidazole rings (Ai et al., 2019; Pan et al., 2011). The bands identified in the region 600 to 800 cm^{-1} are attributed to the out of plane bending of the imidazole ring, and the band closer to 420 cm^{-1} exhibits the stretching vibration of the Zn–N bond (Ai et al., 2019; Cai et al., 2023; Pan et al., 2011).

The characteristic bands of the pristine ZIF-8 dominate all samples spectra. Compared to ZIF-8, $\text{Fe}_3\text{O}_4\text{ZIF-8}$ and $\text{PAA-Fe}_3\text{O}_4\text{ZIF-8}$ composites exhibited two bands at 585 cm^{-1} and 630 cm^{-1} in addition to the characteristic peaks of ZIF-8, which were consistent in the presence of Fe_3O_4 nanoparticles (Cai et al., 2023). The presence of Fe^{2+} was identified in the sample with a higher amount of iron, $\text{Fe}_2\text{ZIF-8}$, by the

existence of the band at 520 cm^{-1} . The appearance of these bands suggests that the incorporation of the different species of iron affected the ZIF-8 structure.

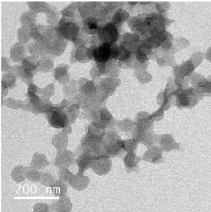
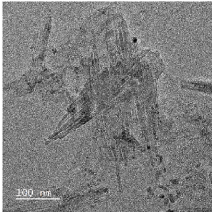
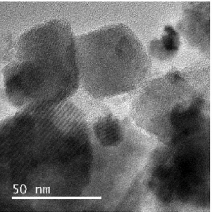
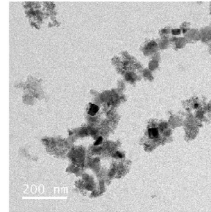
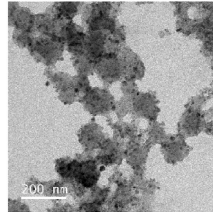
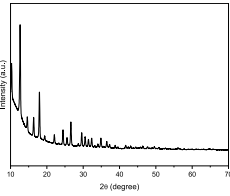
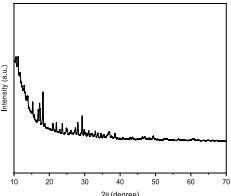
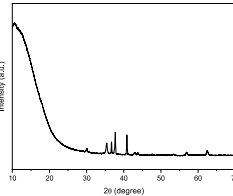
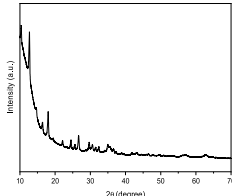
The microstructure of pristine ZIF8 nanoparticles and the samples were obtained by TEM image, and the results have shown that introducing different iron species modifies the average size and shape of the particles. The average size of ZIF-8 was approximately 49.7 nm, with a spherical form in the particles. The introduction of the iron particles in the pristine ZIF-8 modifies the morphology of the structure. In all samples with iron, the little dark spots in the particles detected are attributed to the presence of iron. The spherical particles depend on the iron precursor used in the synthesis. The morphology of both $\text{Fe}_1\text{ZIF-8}$ and $\text{Fe}_2\text{ZIF-8}$ differs from the pristine ZIF-8, with very small particles of iron on the surface. Nevertheless, the modification of the pristine ZIF-8 by introducing Fe_3O_4 and $\text{PAA-Fe}_3\text{O}_4$ seems also to modify the shape of the particles with the increase of their size.

From Table 1, the characteristic peaks of ZIF-8 nanoparticles were observed in the XRD patterns of pristine ZIF-8 and $\text{Fe}_1\text{ZIF-8}$ (Ai et al., 2019; Pan et al., 2011). When the amount of iron is increased in $\text{Fe}_2\text{ZIF-8}$, a reduction of the characteristic peaks of the structure was observed, suggesting that introducing Fe^{2+} into ZIF-8 affects its structure and crystallinity. In addition, the presence of Fe_3O_4 in both samples affects the crystallinity of the ZIF-8 structure, in agreement with FTIR and TEM analyses.

In order to evaluate the catalytic performance of the different synthesized ZIF-8 nanoparticles in the degradation of tartrazine by the Fenton-like reaction, a screening was performed using the experimental conditions described in (Santos et al., 2021). Fig S2 shows the results obtained for the different heterogeneous ZIF-8 catalysts with hydrogen peroxide in terms of Tar conversion, and TOC determined at the end of the reaction (4 h). The pristine catalyst is active in the degradation of Tar, with a conversion of 19.3%, suggesting the Zn participate as active metal in the Fenton-like reaction.

The highest conversion value (35.2%) is obtained with $\text{Fe}_1\text{ZIF-8}$ catalyst, despite the pristine ZIF-8 achieving high mineralization efficiency (17.4%). The presence of Fe_3O_4 nanoparticles increases the conversion but is not efficient in the mineralization, with a Tar conversion of 25.2% and 14.4% for $\text{Fe}_3\text{O}_4\text{ZIF-8}$ and $\text{PAA-Fe}_3\text{O}_4\text{ZIF-8}$, respectively. Between the heterogeneous catalysts with Fe^{2+} , the increase of iron and the decrease of Zn do not favour the conversion of Tar, indicating that the ratio 20:80 Fe/Zn in the catalyst allows the optimal combination for achieving the best catalytic performance. Increasing the amount of Fe in the $\text{Fe}_2\text{ZIF-8}$ catalyst shows that the conversion obtained is similar to that of pristine ZIF-8 nanoparticles, 18.8%. This is explained

Table 1
TEM images and XRD patterns of the synthesized heterogeneous ZIF-8 nanoparticles.

	ZIF-8	$\text{Fe}_1\text{ZIF-8}$	$\text{Fe}_2\text{ZIF-8}$	$\text{Fe}_3\text{O}_4\text{ZIF-8}$	$\text{PAA-Fe}_3\text{O}_4\text{ZIF-8}$
TEM					
XRD				nd	

Nd – not determined.

by the fact that a higher amount of Fe decreases the crystallinity of the sample, as shown in the XRD results (Table 1), which negatively affects the catalytic activity.

So, the Fe₁ZIF-8 catalyst was selected to use in Box-Behnken Design (BBD) model through a matrix of 15 experiments to determine the optimum experimental conditions for efficient oxidation by the data listed in Table S2. Central point conditions ($X_1 = 51$ mM of H₂O₂, $X_2 = 35$ mg, and $X_3 = 4$ h) were run in triplicate for the BBD analysis. The analysis of variance (ANOVA) findings to evaluate the validity of the statistical model testing (Table S3).

In ANOVA, the most parameters tested to assess the model validation are the ratio values of the model's mean-square, the F-values signified and the confidence interval P-values of model terms were computed at 95%, which means that P-value < 5% insured the model's significance (Assila et al., 2023). Hence, the higher F-values (458.97) for Tar conversion in the presence of the catalyst, in addition to the low p-values (<0.001), confirm that the statistical validation had high significance. The mass of catalyst Fe₁ZIF-8 (F-value = 3511.81) was found to be the factor with the largest effect on the Tar conversion efficiency and this was followed by the effect of contact time (F-value = 397.74) and the effect of hydrogen peroxide concentration (F-value = 9.94). However, the large value of lack of fit may simply be missing 18.71% due to noise. Non-significant lack of fit is good, the model to fit. Moreover, the values of correlation coefficients (R^2) for Tar conversion were very high with $R^2 = 0.9988$ and Adj $R^2 = 0.9966$ (Table S3), demonstrating that the application of the developed model is well fitted to the experimental values and highly predictive (Assila et al., 2023; Trovó et al., 2013).

Furthermore, the results illustrated in Fig. 1a and b revealed that a high positive correlation between the predicted and the experimental values of Tar conversion. In addition, the data point on the normal probability plot of the residuals was practically close to a straight line. Indicating that the model is suitable and has a good performance for the response of the Tar degradation by Fenton-like reaction in presence of Fe₁ZIF-8. Accordingly, the second order polynomial relation that allowed determining the regression between the three different factors and the response Tar (Y_1) conversion was expressed by equation (3):

$$Y_1 = 52.64 + 1.04X_1 + 19.5X_2 + 6.56X_3 - 0.15 X_1 X_2 + 5.93 X_1 X_3 + 0.5 X_2 X_3 - 3.31 X_1^2 - 0.5825 X_2^2 - 0.7075X_3^2 \quad (\text{Eq. 3})$$

Where X_1 , X_2 and X_3 correspond to independent variables of the concentration of hydrogen peroxide, the mass of catalyst and the contact time of reaction, respectively. The positive sign in front of the terms

observed the synergistic effect and the negative sign indicates an antagonistic effect (Khouni et al., 2010; Tavares et al., 2009). For the degradation by Fenton-like reaction in the presence of Fe₁ZIF-8, the most important variable is the mass of catalyst, and the interaction between the concentration of hydrogen and the mass of the catalyst is not significant in this case.

Three-dimensional (3D) response surface plots (RSP) for Tar conversion versus concentration of hydrogen peroxide, contact time and mass of catalyst Fe₁ZIF-8 are shown in Fig. 2.

Fig. 2a demonstrate the effect of the initial concentration of H₂O₂ on the Tar degradation and, when changing the concentration from 12 to 90 mM, the differences observed no influence on the reaction rate, which confirms the low interaction between the concentration of hydrogen and the mass of catalyst. To avoid iron leaching, a constant pH = 3.0 was used during the tests (Assila et al., 2023) and the performances of Tar degradation by Fenton-like reaction was achieved at 4 h (Fig. 2b). Concerning the Fe₁ZIF-8 amount used, RSP indicates that the conversion rate reaches the best results with the 50 mg at 40 °C, which is considered suitable for a reaction temperature in order to achieve the best comprise for better degradation (Fig. 2c).

Table S4 shows the optimal experimental conditions by BBD for the degradation of Tar by Fenton-like oxidation in the presence of Fe₁ZIF-8: 50 mg of catalyst (2 g/L), 12 mM of H₂O₂ and 4 h, 30 ppm at $T = 40$ °C and pH = 3, which are degraded and mineralized until 66.50% and 44.17%, respectively.

The adequacy of the proposed mathematical model for Tar degradation by Fenton-like oxidation in the presence of heterogeneous ZIF-8 catalysts was evaluated using the optimum conditions. For this purpose, pristine ZIF-8 and the selected Fe₁ZIF-8 catalyst were used as heterogeneous catalysts to check their contribution to the degradation of Tar by the optimum experimental parameters. As well as, the influence of H₂O₂ as an oxidant in the presence of the Tar was evaluated. Fig. 3 shows the catalytic results obtained under the optimum experimental parameters of the Fenton-like oxidation for Tar using 2 g/L of the catalysts, which significantly agrees with the theoretical values indicated by the mathematical model.

The best catalytic performance was in the presence of Fe₁ZIF-8 with H₂O₂, which proves that the reaction follows the Fenton-like oxidation, with a conversion nearly to 70% in accordance with the conversion predicted by the model (Table S4). Besides, it should also be referred to that the Tar conversions in the presence of H₂O₂ (orange curve) without catalyst and the Fe₁ZIF-8 catalyst without H₂O₂ (blue curve), as control

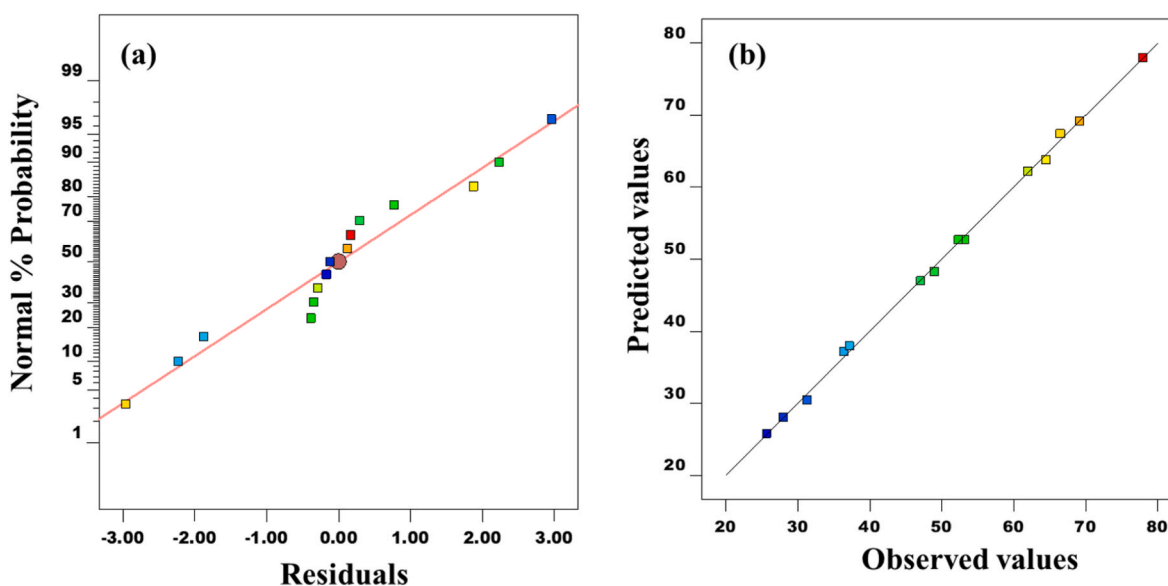


Fig. 1. Normal plot of residuals (a) and predicted values versus actual model values (b) for Tar degradation by Fenton-like reaction in presence of Fe₁ZIF-8.

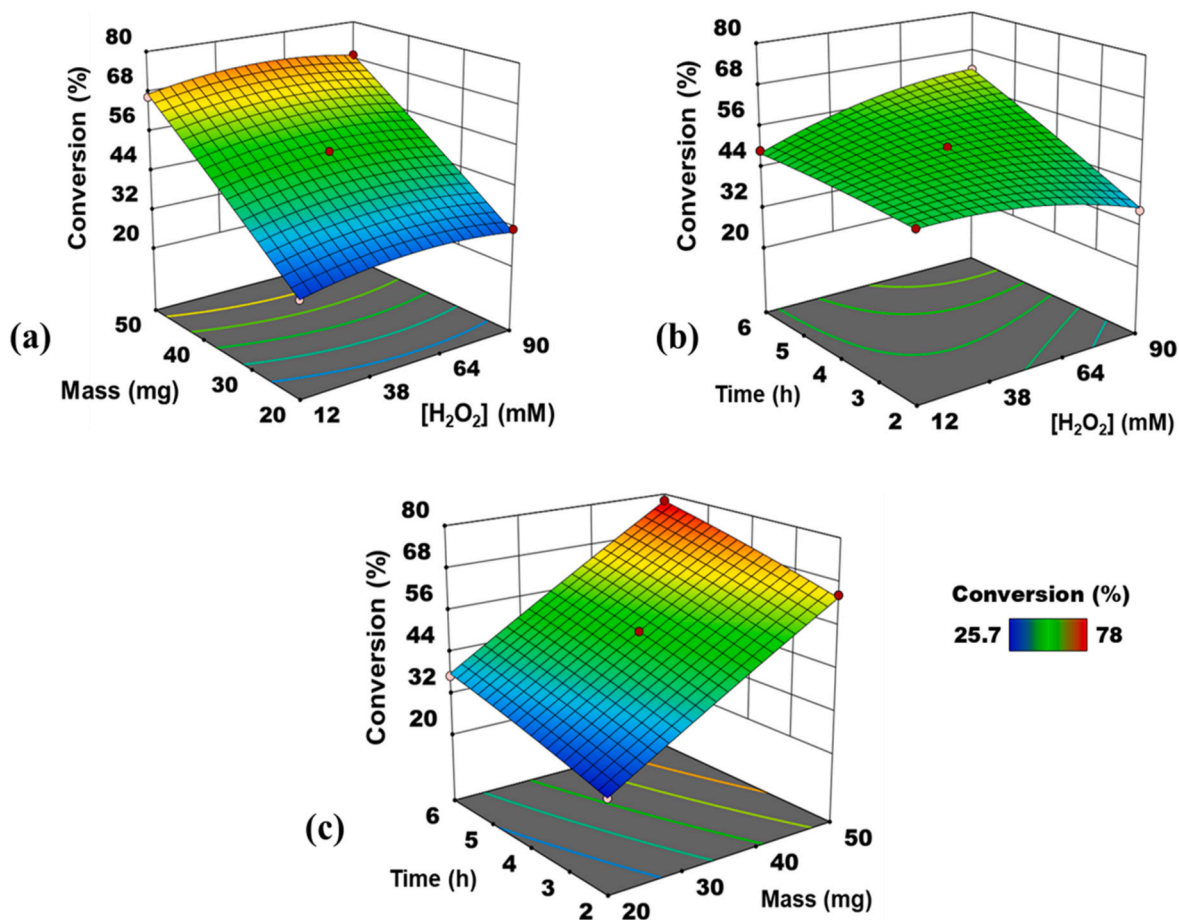


Fig. 2. 3D Response Surface Plots (RSP): Effect of the three variables studied over $\text{Fe}_1\text{ZIF-8}$ in the degradation of Tar by Fenton-like reaction.

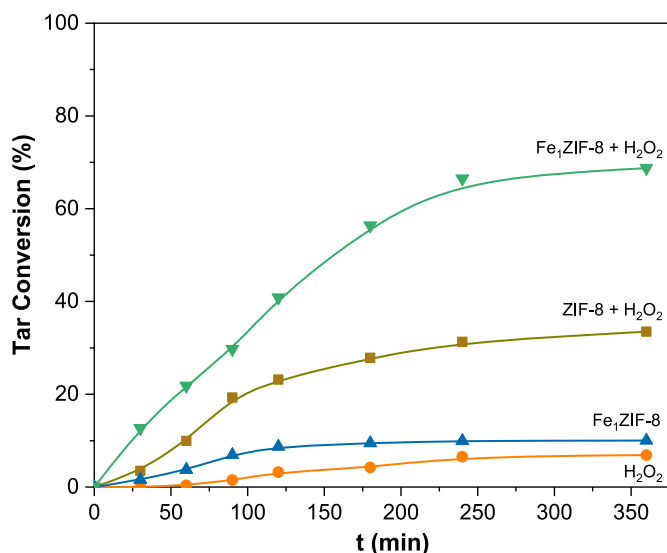


Fig. 3. Conversion of Tar versus reaction time over H_2O_2 (orange curve), pristine ZIF-8 + H_2O_2 (brown curve), $\text{Fe}_1\text{ZIF-8}$ (blue curve) and $\text{Fe}_1\text{ZIF-8}$ + H_2O_2 (green curve). (For interpretation of the references to colour in this figure legend, the reader is referred to the Web version of this article.)

tests, are practically negligible as compared to the pristine ZIF-8 with H_2O (brown curve) and $\text{Fe}_1\text{ZIF-8}$ + H_2O_2 (green curve). On the other hand, the presence of iron in the ZIF-8 framework with H_2O_2 improves the catalytic behaviour and presents a higher conversion rate than

$\text{Fe}_1\text{ZIF-8}$ alone (curve blue). After 240 min of reaction, Tar degradation was 66.5% with a mineralization efficiency of 44.2%, which confirms that the best combination for achieving higher conversions and mineralization was in the presence of $\text{Fe}_1\text{ZIF-8}$ + H_2O_2 catalyst using the optimal experimental conditions determined by BBD model.

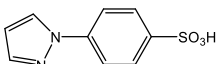
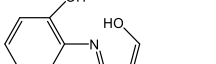
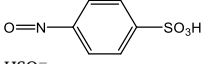
In order to assess the consumption of H_2O_2 during the degradation of Tar by the heterogeneous Fenton process, the quantification of the oxidant was measured by a colorimetric method at the end of the reaction. So, the amount quantified was 4.41 mM, confirming an important reduction of the H_2O_2 (initial concentration, 12 mM) due to the formation of hydroxyl radicals (HO^\bullet) in the Fenton reaction.

Identification of the products during Tar degradation by Fenton-like reaction over $\text{Fe}_1\text{ZIF-8}$ was carried out by HPLC-ESI/MS analysis. This analysis allowed identify several products deriving from the Tar degradation, and proposed the formation of the same intermediate products up to mineralization. The oxidant agents are the OH^\bullet radicals and they are responsible for the formation of the several products identified up to the mineralization. According to the different mass peaks (m/z) obtained in HPLC-ESI/MS chromatograms and ESI-MS/MS spectra in positive and negative modes (Fig. S3), four fragments - two each in positive and negative modes - were identified and are presented in Table 2.

The identified fragment with m/z 223 and 155 suggests that the Tar compound follows a symmetric degradation of the $\text{N}=\text{N}$ azo bond (Dung et al., 2022; Rao et al., 2017; Vu et al., 2019). The attack of the hydroxyl radicals (HO^\bullet) to this bond provokes the symmetric cleavage of the molecule (Muñoz-Flores et al., 2022). In the work of Muñoz-Flores et al. (2022), in their detailed proposed mechanism, the pathway of the $\text{N}=\text{N}$ azo bond by successive attack of HO^\bullet is preferred to form the compounds C1, C2 and C3. To support this statement, it is known that two

Table 2

Summary of fragments identified by ESI-MS/MS after Tar degradation in the presence of Fe₁ZIF-8 catalyst.

Product	<i>m/z</i> (a.m.u)	Structural formula
C1	223	
C2	165	
C3	155	
C4	97	HSO ₄ ⁻

distinct bands characterize the UV/vis spectrum of Tar: a broad band in the visible region at 427 nm, which is attributed to the chromophore groups, and a narrower band in the ultraviolet region at 261 nm, characteristic of the aromatic rings (Rao et al., 2017). At the end of the reaction, the solution becomes colourless and a marked decrease in both characteristic bands of the Tar is observed (Fig S4). The band assigned at 261 nm disappears after 60 min of reaction and the band at 427 nm decreases in intensity, which confirms a symmetric degradation of the azo bond. The disappearance of the absorption maximum band at 261 nm could be attributed to the degradation of compounds with few conjugated groups (Dung et al., 2022; Rao et al., 2017; Vu et al., 2019). In addition, the presence of the fragment HSO₄⁻ (C4) confirms the presence of products from mineralization and results from the total degradation of the pristine compound by the successive attacks of HO[•]. In the presence of Fe₁ZIF-8, the conversion of Tar was 66.5% with a mineralization efficiency of 44.2%, which is very high compared with the heterogeneous catalysts based in zeolites (Assila et al., 2023; Santos et al., 2021).

The catalytic stability and reusability of the Fe₁ZIF-8 catalyst in the Fenton-like degradation of Tart were studied during four successive cycles and at the end of each cycle, TOC was quantified (Fig. 4).

Fig. 4 illustrates that the Fe₁ZIF-8 catalysts showed great stability despite losing the same activity, after the four cycles the catalyst presented a Tar conversion of 59.4%, close to the conversion determined for cycle 1, 66.5%. Remarkably, despite having a slight loss of activity, the catalyst is quite efficient in mineralization. On the other hand, the $X_{\text{Tar}}/\text{TOC}$ ratio remains almost constant during the reusability tests, varying between 1.51 (1^o cycle) and 1.48 (4^o cycle), indicating that the

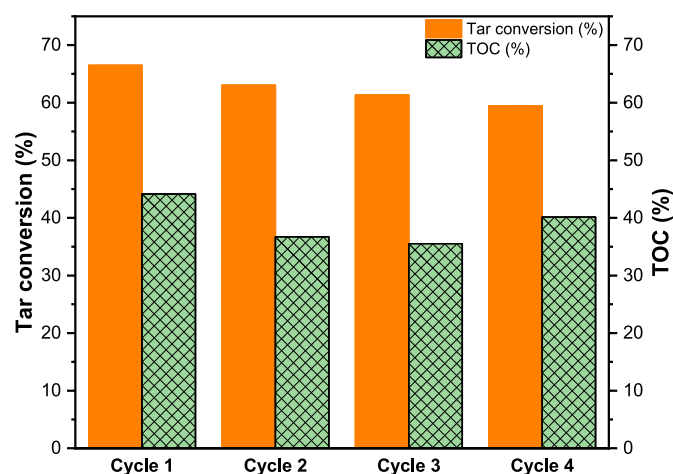


Fig. 4. Conversion and TOC percentages during the consecutive degradation cycles of Tar by Fenton-like reaction in the presence of Fe₁ZIF-8. Conditions of the reaction: 50 mg of catalyst/25 mL at 30 ppm of Tar; 0.5 mL of 12 mM H₂O₂; pH = 3; T = 40 °C and 4 h of reaction.

catalyst maintains its mineralization capacity despite getting worse the degradation performance. These results suggest that the catalyst retained the same catalytic performance for degradation/mineralization during the successful cycles. Furthermore, the slight decrease in activity was likely attributed to the adsorption of compounds as low molecular weight organic acids from the degradation reaction on the catalyst's surface.

FTIR and EDX analyses of the Fe₁ZIF-8 catalyst were performed after Tar degradation at the end of cycle four (Fig S5). After Tar degradation by the Fenton-like reaction, FTIR spectra of the catalyst are similar between cycles 1 and 4, and show the characteristic bands of the pristine ZIF-8 (Fig S1). EDX analysis confirms the presence of the typical elements of the ZIF frameworks, as well as the presence of the iron without leaching. Moreover, the amount of iron 13.5 wt% and 41.9 wt% represent almost 24% of Fe and 76% of Zn in Fe₁ZIF-8, which endorses that the nanoparticles preserved the original ratio of 80 Zn:20 Fe used in the synthesis, indicating that the Fe₁ZIF-8 catalyst possessed excellent stability. These results show that the heterogeneous Fe₁ZIF-8 catalyst has excellent reusability and could be used as an efficient catalyst for degrading pollutants from wastewater by a Fenton-like process.

The effluent treated by Fenton-like degradation was subjected to germination tests with corn seeds using the normalized method to assess toxicity described in the experimental section (Sancey et al., 2011). The results of the germination test were estimated using three different solutions: 30 ppm of the Tar compound untreated, the treated solution of the Tar with Fe₁ZIF-8 by Fenton-like reaction and distilled water (blank), displayed in Fig. 5.

There is a significant difference between the untreated solution and treated Tar solution by Fenton-like reaction using the heterogeneous ZIF-8 catalyst. The germination rate of corn kernels in the Petri dishes irrigated with deionized water for 6 days at room temperature reached 100%, concerning the germination rate in the treated Tar solution using the Fe₁ZIF-8 catalyst was <95% on the sixth day. On the other hand, Fig. 5b shows the high toxicity of untreated Tar solution, which inhibits the corn kernels from germinating and presents a mold proliferation. According to the results, the Fe₁ZIF-8 catalyst by Fenton-like reaction under the optimal experimental conditions clearly decreased the water toxicity allowing the germination of all the corn kernels. Consequently, catalytic oxidation by Fenton-like reaction using heterogeneous ZIF-8 catalysts represents an interesting tool for preventing or decreasing the environmental impact of the contaminated effluents.

4. Conclusions

Iron zeolitic imidazole framework-8 (FeZIF-8) nanoparticles as heterogeneous catalysts were synthesized and evaluated in the degradation of tartrazine (Tar) by the Fenton-like reaction. The optimization of the degradation of Tar by oxidation treatment was achieved through the response surface methodology using Fe₁ZIF-8 as the best catalyst. The stability and reuse of the catalyst were proven and the $X_{\text{Tar}}/\text{TOC}$ ratio remained almost constant during the reusability tests with a high percentage of TOC removal. The high efficiency mineralization observed suggests that the catalyst is able to produce intermediate compounds by the attack of the hydroxyl radicals formed by the Fenton reaction. In addition, germination tests confirmed the efficiency of the degradation of Tar by the Fenton-like process using Fe₁ZIF-8 catalyst to radically decrease the effluent toxicity. The results suggest that using heterogeneous iron ZIF-8 catalysts for catalytic oxidation via a Fenton-like reaction holds great promise in treating contaminated effluents with organic pollutants. Considering that mineralization represents the most desirable outcome, our findings contribute significantly to the search for practical and effective water treatment solutions.

Credit author statement

Ouissal Assila: Formal analysis, Software, Investigation, Writing –

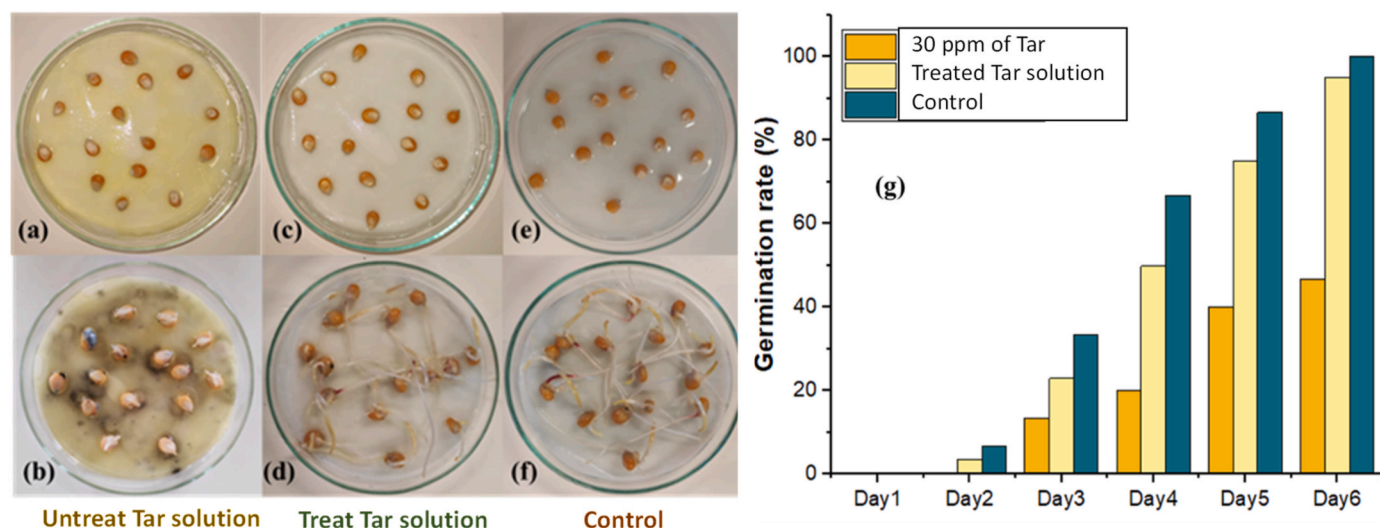


Fig. 5. Images of the germination of corn kernels during 6 days: initial test (day 1) for untreated Tar solution (a), treated Tar solution (c) and control (e); after 6 days for untreated Tar solution (b), treated Tar solution (d) and control (f); and germination rate (%) of (g) in Tar dye untreated (a, b), treated dye (c, d) and blank (e, f).

original draft. Natália Vilaça: Formal analysis, Methodology, Investigation. Ana R. Bertão: Formal analysis, Investigation. Pier Parpot: Software, Methodology, Validation, Writing – review & editing. António M. Fonseca: Validation, Writing – review & editing, Funding acquisition. Olívia S.G.P. Soares: Investigation, Validation, Writing – review & editing. Manuel F.R. Pereira: Validation, Writing – review & editing. Fátima Baltazar: Validation, Writing – review & editing. Manuel Bañobre-López: Conceptualization, Validation, Writing – review & editing, Funding acquisition, Supervision. Isabel C. Neves: Conceptualization, Methodology, Validation, Writing – review & editing, Funding acquisition, Supervision. All authors have read and agreed to the published version of the manuscript.

Declaration of competing interest

The authors declare that they have no known competing financial interests or personal relationships that could have appeared to influence the work reported in this paper. This manuscript is an original work; the results are novel and constitute an important contribution to the water treatment by Fenton processes. The manuscript has not been published previously and is not under consideration for publication elsewhere. The work was written by the stated authors who are all aware of its content and approve its submission. All authors declare do not have a Conflict of Interest.

Data availability

Data will be made available on request.

Acknowledgements

O.A. thanks to ERASMUS + Program for the mobility Ph.D. grant and A.R.B. thanks to Fundação para Ciência e Tecnologia, FCT (Portugal) for her Ph.D. grant (SFRH/BD/141058/2018). This research work has been funded by national funds funded through FCT/MCTES (PIDDAC) over the projects: LA/P/0045/2020 (ALiCE), UIDB/50020/2020 and UIDP/50020/2020 (LSRE-LCM), Centre of Chemistry (UID/QUI/0686/2020), CEB (UIDB/04469/2020) and project BioTecNorte (operation NORTE-01-0145-FEDER-000004), supported by the Northern Portugal Regional Operational Program (NORTE 2020), under the Portugal 2020 Partnership Agreement, through the European Regional Development Fund (ERDF).

Appendix A. Supplementary data

Supplementary data related to this article can be found at <https://doi.org/10.1016/j.chemosphere.2023.139634>.

References

- Alcantara-Cobos, A., Gutiérrez-Segura, E., Solache-Ríos, M., et al., 2020. Tartrazine removal by ZnO nanoparticles and a zeolite-ZnO nanoparticles composite and the phytotoxicity of ZnO nanoparticles. *Microporous Mesoporous Mater.* 302 <https://doi.org/10.1016/j.micromeso.2020.110212>.
- Ai, S., Guo, X., Zhao, L., et al., 2019. Zeolitic imidazolate framework-supported Prussian blue analogues as an efficient Fenton-like catalyst for activation of peroxydisulfate. *Colloids Surfaces A Physicochem. Eng. Asp.* 581, 123796 <https://doi.org/10.1016/j.colsurfa.2019.123796>.
- Arabzadeh, N., Khosravi, A., Mohammadi, A., et al., 2014. Enhanced photodegradation of hazardous tartrazine by composite of nanomolecularly imprinted polymer-nanophotocatalyst with high efficiency. *Desalination Water Treat.* 57, 1–10. <https://doi.org/10.1080/19443994.2014.989414>.
- Assila, O., Barros, Ó., Fonseca, A.M.F., et al., 2023. Degradation of pollutants in water by Fenton-like oxidation over LaFe-catalysts: optimization by experimental design. *Microporous Mesoporous Mater.* 349, 112422 <https://doi.org/10.1016/j.micromeso.2022.112422>.
- Bergaoui, M., Khalfoui, M., Awadallah, -A.F., et al., 2021. A review of the features and applications of ZIF-8 and its derivatives for separating CO₂ and isomers of C₃- and C₄- hydrocarbons. *J. Nat. Gas Sci. Eng.* 96, 104289 <https://doi.org/10.1016/j.jngse.2021.104289>.
- Cai, W., Zhang, W., Chen, Z., 2023. Magnetic Fe₃O₄@ZIF-8 nanoparticles as a drug release vehicle: pH-sensitive release of norfloxacin and its antibacterial activity. *Colloids Surf., B* 223, 113170. <https://doi.org/10.1016/j.colsurfb.2023.113170>.
- Dung, N.T., Duong, L.T., Hoa, N.T., et al., 2022. A comprehensive study on the heterogeneous electro-Fenton degradation of tartrazine in water using CoFe₂O₄/carbon felt cathode. *Chemosphere* 287, 132141. <https://doi.org/10.1016/j.chemosphere.2021.132141>.
- Gao, L., Chen, Q., Gong, T., et al., 2019. Recent advancement of imidazolate framework (ZIF-8) based nanoformulations for synergistic tumor therapy. *Nanoscale* 11 (2019), 21030–21045. <https://doi.org/10.1039/c9nr06558j>.
- Hu, M., Lou, H., Yan, X., et al., 2018. In-situ fabrication of ZIF-8 decorated layered double oxides for adsorption and photocatalytic degradation of methylene blue. *Microporous Mesoporous Mater.* 271, 68–72. <https://doi.org/10.1016/j.micromeso.2018.05.048>.
- Khouni, I., Marrot, B., Amar, R.B., 2010. Decolorization of the reconstituted dye bath effluent by commercial laccase treatment: optimization through response surface methodology. *Chem. Eng. J.* 156, 121–133. <https://doi.org/10.1016/j.cej.2009.10.007>.
- Lee, Y.R., Jang, M.S., Cho, H.Y., et al., 2015. ZIF-8: a comparison of synthesis methods. *Chem. Eng. J.* 271, 276–280. <https://doi.org/10.1016/j.cej.2015.02.094>.
- Liu, Y., Cheng, H., Cheng, M., et al., 2021. The application of Zeolitic imidazolate frameworks (ZIFs) and their derivatives based materials for photocatalytic hydrogen evolution and pollutants treatment. *Chem. Eng. J.* 417 <https://doi.org/10.1016/j.cej.2020.127914>.
- Muñoz-Flores, P., Poon, P.S., Sepulveda, C., et al., 2022. Photocatalytic performance of carbon-containing CuMo-based catalysts under sunlight illumination. *Catalysts* 12, 46. <https://doi.org/10.3390/catal12010046>.

- Ouassif, H., Moujahid, E.M., Lakhale, R., et al., 2020. Zinc-Aluminum layered double hydroxide: high efficient removal by adsorption of tartrazine dye from aqueous solution. *Surface. Interfac.* 18, 100401 <https://doi.org/10.1016/j.surfin.2019.100401>.
- Pan, Y., Liu, Y., Zeng, G., et al., 2011. Rapid synthesis of zeolitic imidazolate framework-8 (ZIF-8) nanocrystals in an aqueous system. *Chem. Commun.* 47, 2071–2073. <https://doi.org/10.1039/c0cc05002d>.
- Rao, M.P., Wu, J.J., Asiri, A.M., et al., 2017. Photocatalytic degradation of tartrazine dye using CuO straw-sheaf-like nanostructures. *Water Sci. Technol.* 75, 1421–1430. <https://doi.org/10.2166/wst.2017.008>.
- Rodrigues, C.S.D., Soares, O.S.G.P., Pereira, M.F.R., et al., 2021. Fenton's oxidation using iron-containing activated carbon as catalyst for degradation of p-nitrophenol in a continuous stirred tank reactor. *J. Water Process Eng.* 44, 102386 <https://doi.org/10.1016/j.jwpe.2021.102386>.
- Sancey, B., Trunfio, G., Charles, J., et al., 2011. Heavy metal removal from industrial effluents by sorption on cross-linked starch: chemical study and impact on water toxicity. *J. Environ. Manag.* 92, 765–772. <https://doi.org/10.1016/j.jenvman.2010.10.033>.
- Santos, B.L.C., Parpot, P., Soares, O.S.G.P., et al., 2021. Fenton-type bimetallic catalysts for degradation of dyes in aqueous solutions. *Catalysts* 11, 32. <https://doi.org/10.3390/catal11010032>.
- Sellers, R.M., 1980. Spectrophotometric determination of hydrogen peroxide using Potassium Titanium(IV) Oxalate. *Analyst* 105, 950–954. <https://doi.org/10.1039/AN9800500950>.
- Sun, H., Yuan, F., Jia, S., et al., 2023. Laccase encapsulation immobilized in mesoporous ZIF-8 for enhancement bisphenol A degradation. *J. Hazard Mater.* 445, 130460 <https://doi.org/10.1016/j.jhazmat.2022.130460>.
- Tavares, A.P.M., Cristóvão, R.O., Loureiro, J.M., et al., 2009. Application of statistical experimental methodology to optimize reactive dye decolourization by commercial laccase. *J. Hazard Mater.* 162, 1255–1260. <https://doi.org/10.1016/j.jhazmat.2008.06.014>.
- Trovó, A.G., Silva, T.F.S., Gomes, O., et al., 2013. Degradation of caffeine by photo-Fenton process: optimization of treatment conditions using experimental design. *Chemosphere* 90, 170–175. <https://doi.org/10.1016/j.chemosphere.2012.06.022>.
- Vu, A.T., Xuan, T.N., Lee, C.H., 2019. Preparation of mesoporous Fe₂O₃-SiO₂ composite from rice husk as an efficient heterogeneous Fenton-like catalyst for degradation of organic dyes. *J. Water Process Eng.* 28, 169–180. <https://doi.org/10.1016/j.jwpe.2019.01.019>.
- Wang, Z., Lai, C., Qin, L., et al., 2020. ZIF-8-modified MnFe₂O₄ with high crystallinity and superior photo-Fenton catalytic activity by Zn-O-Fe structure for TC degradation. *Chem. Eng. J.* 392, 124851 <https://doi.org/10.1016/j.cej.2020.124851>.
- Zhang, H., Zhou, C., Zeng, H., et al., 2021. ZIF-8 assisted synthesis of magnetic core-shell Fe₃O₄@CuS nanoparticles for efficient sulfadiazine degradation via H₂O₂ activation: performance and mechanism. *J. Colloid Interface Sci.* 594, 502–512. <https://doi.org/10.1016/j.jcis.2021.03.057>.
- Zhou, X., Zhang, H.P., Wang, G.Y., et al., 2013. Zeolitic imidazolate framework as efficient heterogeneous catalyst for the synthesis of ethyl methyl carbonate. *J. Mol. Catal. A: Chem.* 366, 43–47. <https://doi.org/10.1016/j.molcata.2012.09.006>.